

Electronic Supplementary Information

Analysis of factors governing the formation of single-stranded helical coordination polymers from a macrocyclic metalloligand and Ca^{2+} , Mn^{2+} , Fe^{2+} , Co^{2+} , Ni^{2+} , Cu^{2+} , Zn^{2+} and Pb^{2+}

Xiao-Zeng Li,* Peng-Peng Hao, Dan Wang and Li-Na Zhu

Department of Chemistry, Tianjin University, Tianjin 300072, P. R. China

Email: lixiaozeng321@tju.edu.cn, Tel: +86 022 27403475

Materials and Measurements. All starting materials and solvents were purchased commercially and were used as received. $[\text{Na}_8(\text{NiL}^1)_4(\text{C}_2\text{H}_5\text{OH})_6(\text{H}_2\text{O})_{16}] \cdot 2\text{H}_2\text{O}$ was prepared according to the method previously reported by us.¹ Infrared spectra were obtained from KBr pellets on a BIO-RAD 3000 infrared spectrophotometer in the 400-4000 cm^{-1} region. Elemental analyses of C, H and N were determined with a Perkin-Elmer 240 Elemental Analyzer. Thermogravimetric analyses (TGA) were carried out in nitrogen stream using a STA-409PC equipment at a heating rate of 10 $^\circ\text{C}/\text{min}$. Powder X-ray diffraction (PXRD) data were recorded on a Rigaku D/max 2500v/pc X-ray powder diffractometer ($\text{Cu K}\alpha$, 1.5418 Å).

Synthesis of $\{[\text{Co}(\text{NiL}^1)(\text{C}_2\text{H}_5\text{OH})(\text{CH}_3\text{OH})(\text{H}_2\text{O})] \cdot \text{CH}_3\text{OH}\}_n$ (1). A mixture of $[\text{Na}_8(\text{NiL}^1)_4(\text{C}_2\text{H}_5\text{OH})_6(\text{H}_2\text{O})_{16}] \cdot 2\text{H}_2\text{O}$ (0.040 g, 0.0141 mmol), $\text{Co}(\text{ClO}_4)_2 \cdot 6\text{H}_2\text{O}$ (0.0210 g, 0.0574 mmol), ethanol (25 ml), methanol (80 ml) and water (60 ml) was stirred to form a red solution. The filtrate of the solution was then stored at room temperature for 7 days, and red crystals suitable for X-ray single crystal analysis were formed. Yield: 0.0183 g (46.5%, calculated on the amount of $[\text{Na}_8(\text{NiL}^1)_4(\text{C}_2\text{H}_5\text{OH})_6(\text{H}_2\text{O})_{16}] \cdot 2\text{H}_2\text{O}$). Anal. Calc. for $\text{C}_{28}\text{H}_{28}\text{CoN}_4\text{NiO}_{10}$: C 48.17, H 4.04, N 8.02%. Found: C 48.28, H 4.05, N 8.06%. IR (KBr, cm^{-1}): 3577(s), 3050(m), 2888(m), 1605(s), 1581(s), 1536(s), 1440(m), 1380(s), 1347(m), 752(m).

Synthesis of $\{[\text{Cu}(\text{NiL}^1)(\text{H}_2\text{O})_3] \cdot 3\text{H}_2\text{O}\}_n$ (2). A mixture of $[\text{Na}_8(\text{NiL}^1)_4(\text{C}_2\text{H}_5\text{OH})_6(\text{H}_2\text{O})_{16}] \cdot 2\text{H}_2\text{O}$ (0.0690 g, 0.0242 mmol), $\text{CuSO}_4 \cdot 5\text{H}_2\text{O}$ (0.0245 g, 0.0981 mmol), water (140 ml) and DMF (18 ml)

was stirred to form a deep red solution. The filtrate of the solution was then stored at room temperature for 7 days, and red crystals suitable for X-ray single crystal analysis were formed. Yield: 0.0295 g (44.6%, calculated on the amount of $[\text{Na}_8(\text{NiL}^1)_4(\text{C}_2\text{H}_5\text{OH})_6(\text{H}_2\text{O})_{16}] \cdot 2\text{H}_2\text{O}$). Anal. Calc. for $\text{C}_{24}\text{H}_{24}\text{N}_4\text{CuNiO}_{12}$: C 42.22, H 3.54, N 8.21%. Found: C 42.33, H 3.55, N 8.22%. IR (KBr, cm^{-1}): 3577(s), 3064(m), 2881(m), 1602(s), 1587(s), 1540(s), 1440(m), 1382(s), 1350(m), 755(s).

Synthesis of $\{[\text{Mn}(\text{NiL}^1)(\text{H}_2\text{O})_3] \cdot 3\text{H}_2\text{O}\}_n$ (3). A mixture of $[\text{Na}_8(\text{NiL}^1)_4(\text{C}_2\text{H}_5\text{OH})_6(\text{H}_2\text{O})_{16}] \cdot 2\text{H}_2\text{O}$ (0.060 g, 0.0211 mmol), $\text{Mn}(\text{ClO}_4)_2 \cdot 6\text{H}_2\text{O}$ (0.0363 g, 0.1003 mmol), water (60 ml) and methanol (60 ml) was stirred to form a deep red solution. The filtrate of the solution was then stored at room temperature for 7 days, and red crystals suitable for X-ray single crystal analysis were formed. Yield: 0.0360 g (63.3%, calculated on the amount of $[\text{Na}_8(\text{NiL}^1)_4(\text{C}_2\text{H}_5\text{OH})_6(\text{H}_2\text{O})_{16}] \cdot 2\text{H}_2\text{O}$). Anal. Calc. for $\text{C}_{24}\text{H}_{24}\text{N}_4\text{MnNiO}_{12}$: C 42.76, H 3.59, N 8.31%. Found: C 43.12, H 3.30, N 8.13%. IR (KBr, cm^{-1}): 3575(m), 3062(m), 2883(m), 1602(s), 1585(s), 1538(s), 1446(m), 1381(s), 1350(m), 751(s).

Crystallography for 1. The diffraction data were collected with a Bruker SMART CCD area detector using graphite-monochromated Mo $K\alpha$ radiation ($\lambda = 0.71073 \text{ \AA}$) with ω and φ scans. Absorption corrections were carried out utilizing SADABS routine.² The structures were solved by the direct methods and refined by full-matrix least-squares refinements based on F^2 .³ Crystal data of **1**: $\text{C}_{28}\text{H}_{28}\text{CoN}_4\text{NiO}_{10}$, $M_r = 698.18$, $T = 293(2) \text{ K}$, monoclinic $P2_1/c$, $a = 16.091(12) \text{ \AA}$, $b = 8.987(6) \text{ \AA}$, $c = 24.710(13) \text{ \AA}$, $\beta = 128.62(3)^\circ$, $V = 2792(3) \text{ \AA}^3$, $Z = 4$, $D_c = 1.661 \text{ g cm}^{-3}$, $\mu = 1.336 \text{ mm}^{-1}$, $R_{\text{int}} = 0.1002$, final $R_1 = 0.0517$, $wR_2 = 0.1763$, $S = 1.040$.

Crystallography for 2. The diffraction data were collected with a Rigaku Saturn CCD area detector using graphite-monochromated Mo $K\alpha$ radiation ($\lambda = 0.71073 \text{ \AA}$) with ω and φ scans. Absorption corrections were carried out utilizing CrystalClear routine.⁴ The structures were solved by the direct methods and refined by full-matrix least-squares refinements based on F^2 .³ Crystal data of **2**: $\text{C}_{24}\text{H}_{24}\text{N}_4\text{CuNiO}_{12}$, $M_r = 682.72$, $T = 113(2) \text{ K}$, monoclinic $P2_1/n$, $a = 15.674(3) \text{ \AA}$, $b = 8.6916(17) \text{ \AA}$, $c = 19.060(4) \text{ \AA}$, $\beta = 91.30(3)^\circ$, $V = 2595.9(9) \text{ \AA}^3$, $Z = 4$, $D_c = 1.747 \text{ g cm}^{-3}$, $\mu = 1.619 \text{ mm}^{-1}$, $R_{\text{int}} = 0.0363$, final $R_1 = 0.0333$, $wR_2 = 0.0945$, $S = 1.100$.

Crystallography for 3. The diffraction data were collected with a Bruker P4/CCD diffractometer using graphite-monochromated Mo K α radiation ($\lambda = 0.71073 \text{ \AA}$) with ω scans. Absorption corrections were carried out utilizing SADABS routine.² The structures were solved by the direct methods and refined by full-matrix least-squares refinements based on F^2 .³ Crystal data of **3**: C₂₄H₂₄N₄MnNiO₁₂, $M_r = 674.10$, $T = 293(2) \text{ K}$, monoclinic $P2_1/c$, $a = 15.90(2) \text{ \AA}$, $b = 8.875(11) \text{ \AA}$, $c = 24.97(2) \text{ \AA}$, $\beta = 128.93(5)^\circ$, $V = 2741(5) \text{ \AA}^3$, $Z = 4$, $D_c = 1.633 \text{ g cm}^{-3}$, $\mu = 1.218 \text{ mm}^{-1}$, $R_{\text{int}} = 0.1004$, final $R_1 = 0.0894$, $wR_2 = 0.2940$, $S = 1.064$.

References

- 1 X.-Z. Li, P.-P. Hao, D. Wang, W.-Q. Zhang and L.-N. Zhu, *CrystEngComm*, 2012, **14**, 366.
- 2 G. M. Sheldrick, SADABS, Program for Empirical Absorption Correction of Area Detector Data. University of Göttingen, Germany, 1996.
- 3 G. M. Sheldrick, SHELXL-97, program for the refinement of the crystal structures. University of Göttingen, Germany, 1997.
- 4 Crystal Structure 3.7.0 and Crystalclear 1.36: Crystal Structure Analysis Package. Rigaku and Rigaku/MS (2000-2005), The Woodlands, TX.

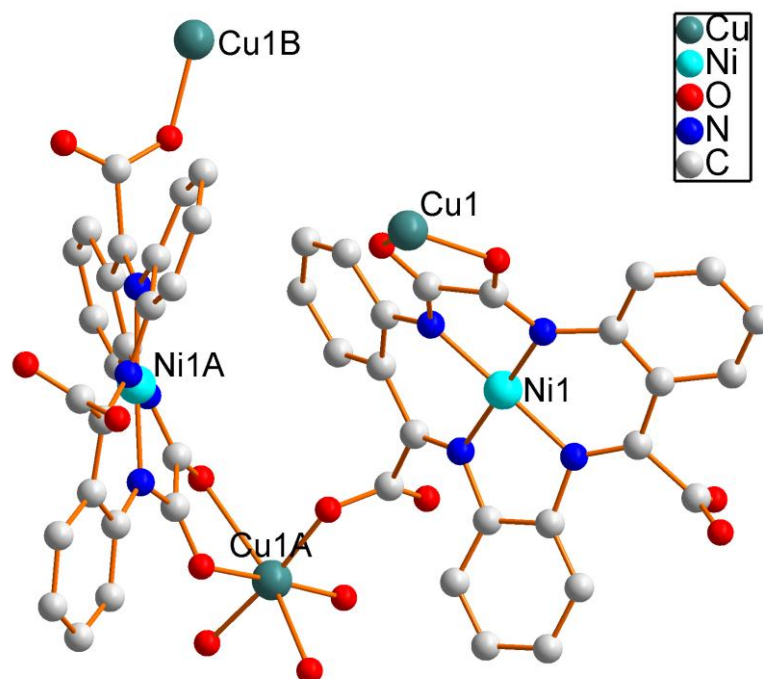


Fig. S1 Plot showing the coordination environments of Ni and Cu atoms, and the coordination mode, “head-to-tail” arrangement and saddle shape of NiL¹ in **2**. (Hydrogen atoms and coordinated solvent molecules have been omitted for clarity.)

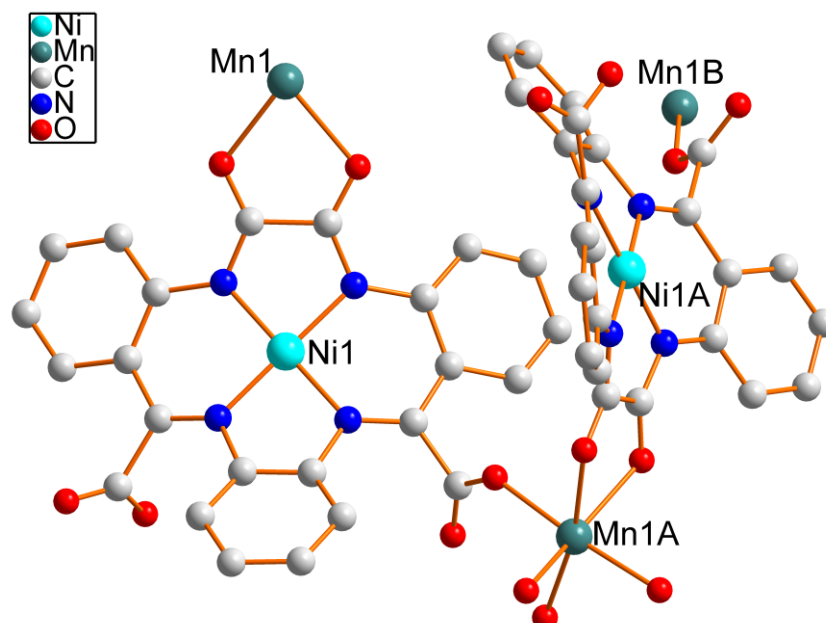


Fig. S2 Plot showing the coordination environments of Ni and Mn atoms, and the coordination mode, “head-to-tail” arrangement and saddle shape of NiL¹ in **3**. (Hydrogen atoms and coordinated solvent molecules have been omitted for clarity.)

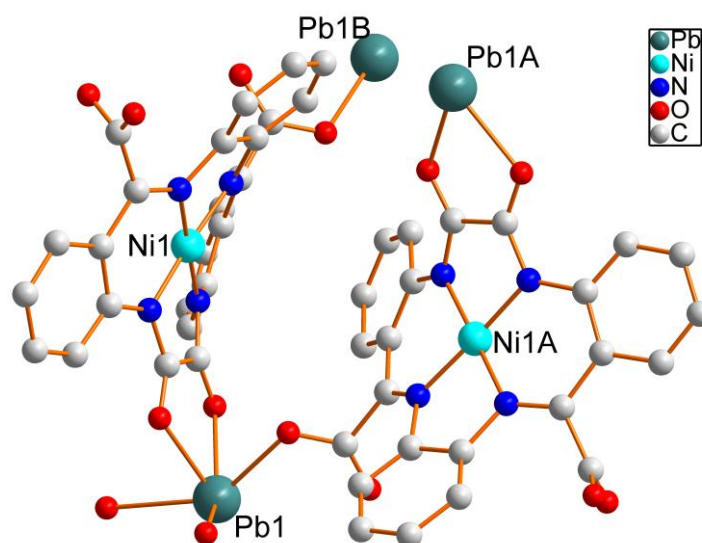


Fig. 3 Plot showing the coordination environments of Ni and Pb atoms, and the coordination mode, “head-to-tail” arrangement and saddle shape of NiL^1 in Pb-NiL^1 . (Hydrogen atoms and coordinated solvent molecules have been omitted for clarity.)

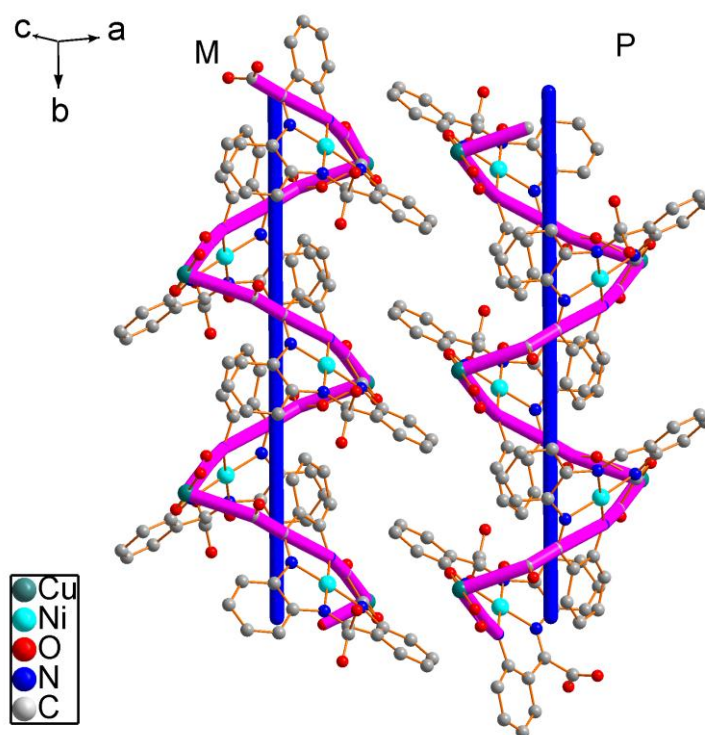


Fig. S4 Left- (M) and right-handed (P) helical chains in **2**. (Hydrogen atoms and coordinated solvent molecules have been omitted for clarity.)

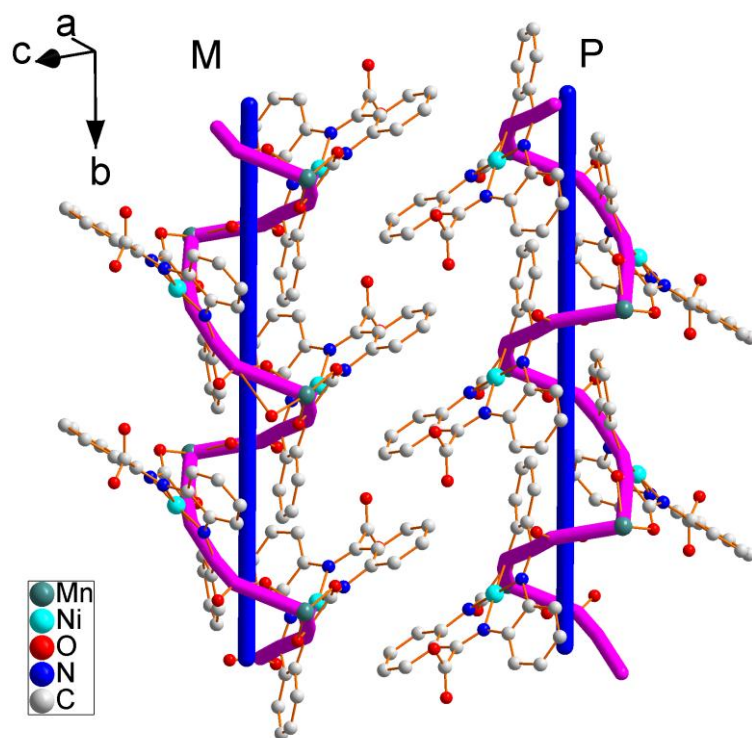


Fig. S5 Left- (M) and right-handed (P) helical chains in **3**. (Hydrogen atoms and coordinated solvent molecules have been omitted for clarity.)

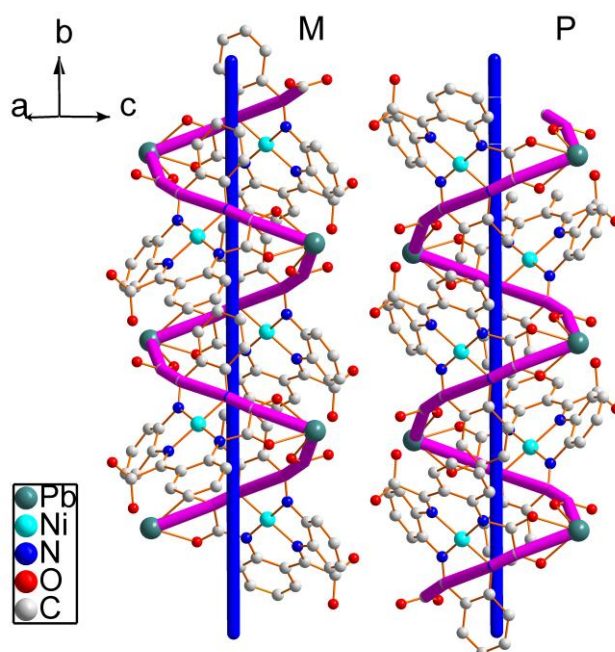


Fig. S6 Left- (M) and right-handed (P) helical chains in Pb-NiL^1 . (Hydrogen atoms and coordinated solvent molecules have been omitted for clarity.)

Table S1 Dihedral angles (°) between mean planes of every NiL¹ ligand in **1–3** and the reported compounds containing NiL¹.

Complex code	Formula	Angle 1 ^a	Angle 2 ^b	Angle 3 ^c
1	{[Co(NiL ¹)(C ₂ H ₅ OH)(CH ₃ OH)(H ₂ O)]·CH ₃ OH} _n	129.3 (1)	132.7(1)	61.2(2), 57.2(5)
2	{[Cu(NiL ¹)(H ₂ O) ₃]·3H ₂ O} _n	129.86(6)	135.12(6)	58.40(6), 57.2(5)
3	{[Mn(NiL ¹)(H ₂ O) ₃]·3H ₂ O} _n	130.2(3)	133.9(3)	59.0(3), 56.8(9)
Fe-NiL ¹	{[Fe(NiL ¹)(CH ₃ OH)(H ₂ O) ₂] ₄ ·3CH ₃ OH·5H ₂ O} _n ^d	130.57(7)	134.16(8)	60.56(8), 57.4(2)
Ni-NiL ¹	{[Ni(NiL ¹)(H ₂ O) ₃]·C ₂ H ₅ OH·2H ₂ O} _n ^d	128.89(7)	133.04(8)	59.85(8), 67.5(3)
Zn-NiL ¹	{[Zn ₂ (NiL ¹) ₂ (H ₂ O) ₆]·8H ₂ O} _n ^d	127.4(2)	132.1(2)	60.6(2), 59.4(2), 127.9(2)
Pb-NiL ¹	{[Pb(NiL)(H ₂ O) ₂]·3H ₂ O} _n ^e	127.8(2)	135.0(3)	57.4(2), 63.3(2)
Ca-NiL ¹	{[Ca(NiL)(H ₂ O) ₄]·3H ₂ O} _n ^e	119.8(2)	134.5(2)	62.5(3), 66.1(4)
Na-NiL ¹	[Na ₈ (NiL ¹) ₄ (C ₂ H ₅ OH) ₆ (H ₂ O) ₁₆]·3H ₂ O ^d	123.9(2)	129.6(2)	63.9(3), 63.2(2)
		137.3(2)	141.1(2)	57.2(5), 55.5(3)
Cd-NiL ¹ -A	{[Cd(NiL ¹)(H ₂ O) ₂]·2DMF} _n ^d	118.7(4)	125.9(4)	64.9(1), 55.3(1)
Cd-NiL ¹ -B	{[Cd(NiL ¹)(C ₂ H ₅ OH)] ₂ ·H ₂ O} _n ^d	136.4(2)	134.4(2)	66.5(5), 63.8(3)

a. The dihedral angle between the plane defined by the oxamido group and the phenyl ring opposite to it.

b. The dihedral angle between the two phenyl rings opposite to each other.

c. The dihedral angle between the plane determined by every carboxylate group and the NiN₄ plane.

d. See: X.-Z. Li, P.-P. Hao, D. Wang, W.-Q. Zhang and L.-N. Zhu, *CrystEngComm*, 2012, **14**, 366.

e. See: X.-J. Kong, X.-Z. Li, S. Ren and L.-N. Zhu, *J. Coord. Chem.*, 2012, **65**, 3641.

Table S2 Atom-to-atom distances (Å) shorter than 3.80 Å between the $\pi\cdots\pi$ interacting NiL¹ ligands in the helical chains of Ca-NiL¹.

C1...C44	3.543(1)	C4...C39 ^a	3.4746(9)
C1...C45	3.676(1)	C4...C40 ^a	3.3543(9)
C2...C43	3.513(1)	C4...N8 ^a	3.399(1)
C5...C32	3.629(1)	C4...Ni2 ^a	3.773(1)
C5...O9	3.729(1)	C5...C35 ^a	3.531(1)
C6...C27	3.490(1)	C5...C40 ^a	3.5217(9)
C6...C28	3.633(1)	C5...N7 ^a	3.722(1)
C6...C29	3.746(1)	C5...N8 ^a	3.749(1)
C6...C30	3.734(1)	C5...Ni2 ^a	3.579(1)
C6...C31	3.5561(8)	C6...C26 ^a	3.670(1)
C6...C32	3.453(1)	C7...C25 ^a	3.514(1)
C7...C27	3.552(1)	C7...C26 ^a	3.556(1)
C7...C28	3.546(1)	C7...O11 ^a	3.6245(9)
C11...C46	3.5090(8)	C7...O12 ^a	3.650(1)
C11...C47	3.3375(8)	C8...C25 ^a	3.527(1)
C12...C47	3.4669(9)	C8...O11 ^a	3.441(1)
C16...C46	3.526(1)	C9...O11 ^a	3.346(1)
N3...C47	3.393(1)	N3...O11 ^a	3.734(1)
N3...C46	3.748(1)	C19...C45 ^a	3.438(1)
N4...C46	3.754(1)	C19...C46 ^a	3.607(1)
O1...C44	3.636(1)	C20...C45 ^a	3.5574(8)
O2...C41	3.354(1)	C21...C45 ^a	3.720(1)
O2...C43	3.434(1)	C22...C45 ^a	3.749(1)
O2...C44	3.6108(9)	C23...C44 ^a	3.546(1)
O2...N8	3.737(1)	C23...C45 ^a	3.625(1)
		C24...C44 ^a	3.553(1)
		C24...C45 ^a	3.469(1)

^a -1+x, y, z

Table S3 Atom-to-atom distances (Å) shorter than 3.80 Å between the $\pi\cdots\pi$ interacting NiL¹ ligands in the helical chains of **1**.

C21...C13 ^a	3.693(7)	C12...C22 ^b	3.646(6)
C22...C12 ^a	3.646(6)	C13...C21 ^b	3.693(7)
C22...C13 ^a	3.520(7)	C13...C22 ^b	3.520(7)
C22...C17 ^a	3.661(6)	C17...C22 ^b	3.661(6)
C22...O6 ^a	3.400(7)	C17...C23 ^b	3.675(6)
C22...N4 ^a	3.565(5)	C19...C23 ^b	3.799(6)
C23...C17 ^a	3.675(6)	C20...C23 ^b	3.779(6)
C23...C19 ^a	3.799(6)	N1...C23 ^b	3.764(7)
C23...C20 ^a	3.779(6)	N4...C22 ^b	3.565(5)
C23...N1 ^a	3.764(7)	N4...C23 ^b	3.725(6)
C23...N4 ^a	3.725(6)	C22...O6 ^b	3.400(7)

^a -x, -0.5+y, 1.5-z; ^b -x, 0.5+y, 1.5-z

Table S4 Atom-to-atom distances (Å) shorter than 3.80 Å between the $\pi\cdots\pi$ interacting NiL¹ ligands in the helical chains of **2**.

C20...C22 ^a	3.678(3)	C15...C22 ^b	3.622(3)
C20...O2 ^a	3.755(3)	C16...C22 ^b	3.734(3)
C20...N4 ^a	3.752(3)	C17...C21 ^b	3.688(3)
C21...C17 ^a	3.688(3)	C17...C22 ^b	3.526(3)
C21...C19 ^a	3.676(3)	C19...C21 ^b	3.676(3)
C21...N3 ^a	3.762(3)	C22...C20 ^b	3.678(3)
C21...N4 ^a	3.584(3)	N3...C21 ^b	3.762(3)
C22...C15 ^a	3.622(3)	N3...C22 ^b	3.516(3)
C22...C16 ^a	3.734(3)	N4...C20 ^b	3.752(3)
C22...C17 ^a	3.526(3)	N4...C21 ^b	3.584(3)
C22...N3 ^a	3.516(3)	O2...C20 ^b	3.755(3)
C22...O6 ^a	3.307(3)	O6...C22 ^b	3.307(3)

^a 1.5-x, 0.5+y, 0.5-z; ^b 1.5-x, -0.5+y, 0.5-z

Table S5 Atom-to-atom distances (Å) shorter than 3.80 Å between the $\pi\cdots\pi$ interacting NiL¹ ligands in the helical chains of **3**.

C18...C23 ^a	3.73(2)	C13...C20 ^b	3.62(1)
C18...O1 ^a	3.71(2)	C13...C21 ^b	3.70(1)
C19...C22 ^a	3.60(2)	C14...C20 ^b	3.75(1)
C19...C17 ^a	3.75(1)	C15...C20 ^b	3.57(1)
C20...C13 ^a	3.62(1)	C17...C19 ^b	3.75(1)
C20...C14 ^a	3.75(1)	C22...C19 ^b	3.60(2)
C20...C15 ^a	3.57(1)	C23...C18 ^b	3.73(2)
C20...N3 ^a	3.52(1)	N3...C20 ^b	3.52(1)
C20...O6 ^a	3.46(1)	O1...C18 ^b	3.71(2)
C21...C13 ^a	3.70(1)	O6...C20 ^b	3.46(1)

^a 2-x, -0.5+y, 0.5-z; ^b 2-x, 0.5+y, 0.5-z

Table S6 Atom-to-atom distances (Å) shorter than 3.80 Å between the $\pi\cdots\pi$ interacting NiL¹ ligands in the helical chains of Fe-NiL¹.

C15...C22 ^a	3.484(3)	O6...C22 ^a	3.349(3)
C15...C23 ^a	3.649(4)	O6...C21 ^a	3.791(3)
C16...C22 ^a	3.628(3)	C21...C17 ^b	3.616(3)
C17...C21 ^a	3.616(3)	C21...C19 ^b	3.738(4)
C17...C22 ^a	3.621(4)	C21...C24 ^b	3.736(4)
C19...C21 ^a	3.738(4)	C21...N3 ^b	3.680(3)
C24...C21 ^a	3.736(4)	C21...N4 ^b	3.764(3)
N3...C21 ^a	3.680(3)	C21...O6 ^b	3.791(3)
N3...C22 ^a	3.545(3)	C22...C15 ^b	3.484(3)
N4...C21 ^a	3.764(3)		

^a 1.5-x, 0.5+y, 0.5-z; ^b 1.5-x, -0.5+y, 0.5-z

Table S7 Atom-to-atom distances (Å) shorter than 3.80 Å between the $\pi\cdots\pi$ interacting NiL¹ ligands in the helical chains of Ni-NiL¹.

C5...C2 ^a	3.727(5)	C2...C5 ^b	3.727(5)
C5...O2 ^a	3.722(5)	C2...O5 ^b	3.722(5)
C6...C3 ^a	3.647(5)	C3...C6 ^b	3.647(5)
C6...C9 ^a	3.764(4)	C9...C6 ^b	3.764(4)
C6...N2 ^a	3.635(5)	C9...C7 ^b	3.668(4)
C7...C9 ^a	3.668(4)	C11...C7 ^b	3.758(4)
C7...O3 ^a	3.442(3)	C16...C7 ^b	3.654(3)
C7...N3 ^a	3.580(4)	N2...C6 ^b	3.635(5)
C7...C11 ^a	3.758(4)	N3...C7 ^b	3.580(4)
C7...C16 ^a	3.654(3)	O3...C7 ^b	3.442(3)

^a -x, 0.5+y, 1.5-z; ^b -x, -0.5+y, 1.5-z

Table S8 Atom-to-atom distances (Å) shorter than 3.80 Å between the $\pi\cdots\pi$ interacting NiL¹ ligands in the helical chains of Zn-NiL¹.

C21...N6	3.752(8)	C1...C31 ^a	3.723(9)
C21...C27	3.659(9)	C15...C28 ^a	3.787(9)
C21...C32	3.716(9)	C15...C29 ^a	3.552(9)
C21...C33	3.649(9)	C16...C29 ^a	3.609(9)
C21...O10	3.684(8)	C17...C29 ^a	3.515(9)
C22...C33	3.694(9)	C17...C30 ^a	3.607(9)
C22...O10	3.285(8)	C19...C30 ^a	3.693(9)
C22...C35	3.625(9)	C24...C30 ^a	3.632(9)
C22...N7	3.699(8)	N4...C29 ^a	3.452(8)
		O1...C31 ^a	3.698(9)

^a -1.5+x, y, z

Table S9 Atom-to-atom distances (Å) shorter than 3.80 Å between the $\pi\cdots\pi$ interacting NiL¹ ligands in the helical chains of Pb-NiL¹.

C6...C22 ^a	3.60(1)	C2...N2 ^b	3.62(1)
C8...C5 ^a	3.66(1)	C5...C8 ^b	3.66(1)
C8...C19 ^a	3.74(1)	C7...C9 ^b	3.61(1)
C9...C7 ^a	3.61(1)	C7...N2 ^b	3.75(1)
C12...C19 ^a	3.56(1)	C7...O2 ^b	3.55(1)
C12...C22 ^a	3.72(1)	C19...C8 ^b	3.74(1)
N2...C2 ^a	3.62(1)	C19...C12 ^b	3.56(1)
N2...C7 ^a	3.75(1)	C19...N3 ^b	3.63(1)
N3...C19 ^a	3.63(1)	C19...O6 ^b	3.27(1)
O2...C7 ^a	3.55(1)	C22...C6 ^b	3.60(1)
O6...C19 ^a	3.27(1)	C22...C12 ^b	3.72(1)

^a 2-x, -0.5+y, 0.5-z; ^b 2-x, 0.5+y, 0.5-z

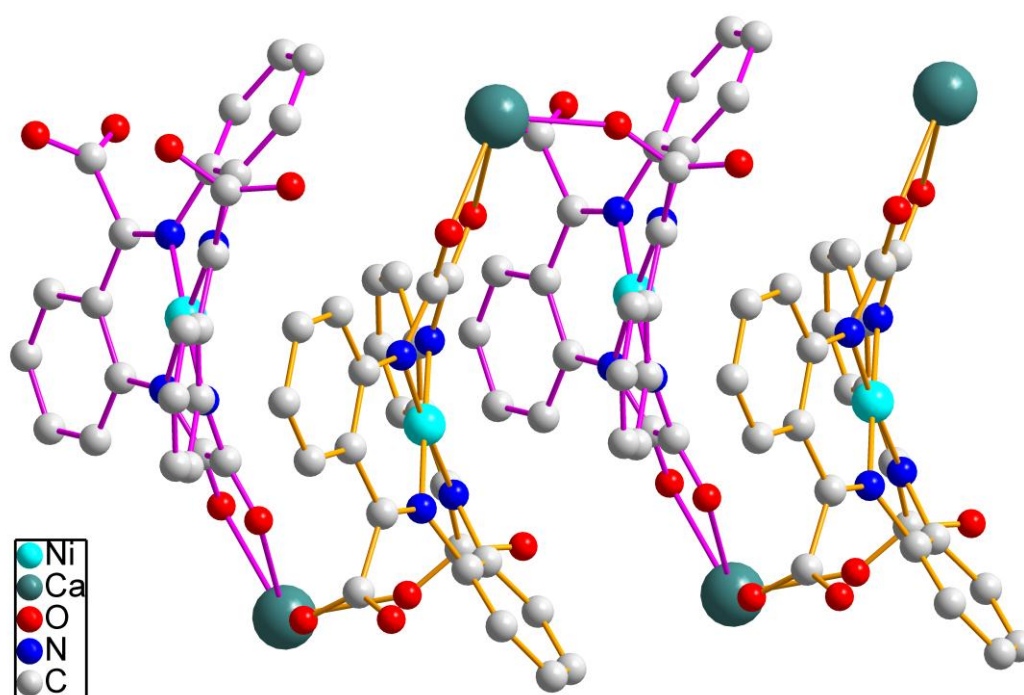


Fig. S7 Plot showing the $\pi\cdots\pi$ interactions between the adjacent NiL¹ ligands in a helical chain of

Ca-NiL¹. (Hydrogen atoms and coordinated solvent molecules have been omitted for clarity.)

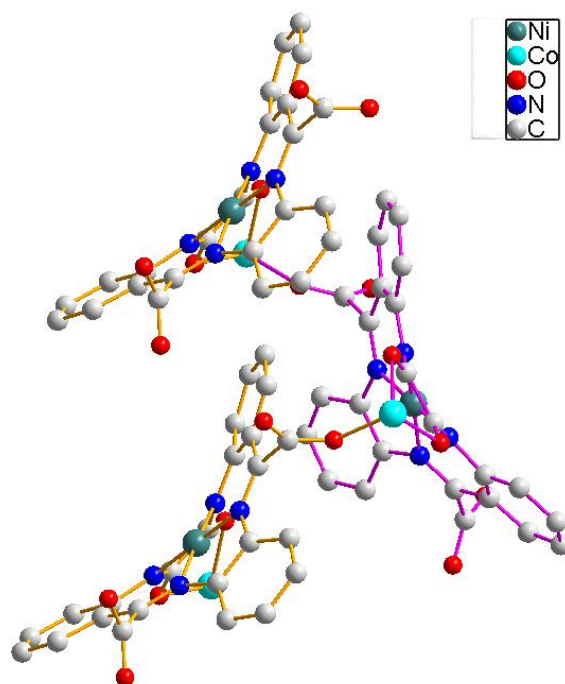


Fig. S8 Plot showing the $\pi \cdots \pi$ interactions between the adjacent NiL¹ ligands in a helical chain of 1. (Hydrogen atoms and coordinated solvent molecules have been omitted for clarity.)

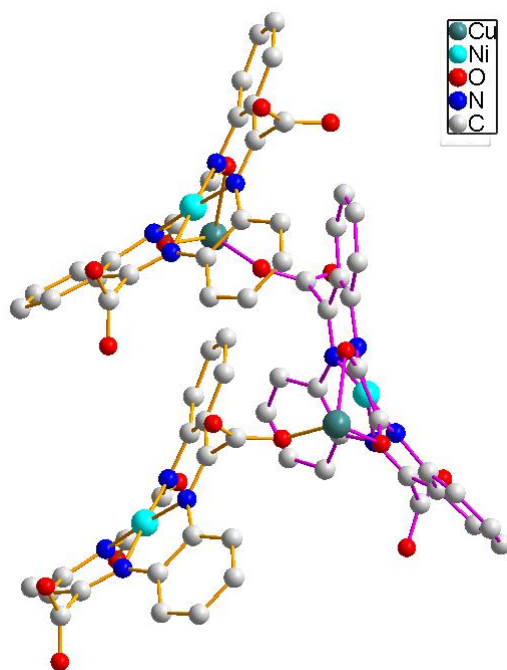


Fig. S9 Plot showing the $\pi \cdots \pi$ interactions between the adjacent NiL¹ ligands in a helical chain of 2. (Hydrogen atoms and coordinated solvent molecules have been omitted for clarity.)

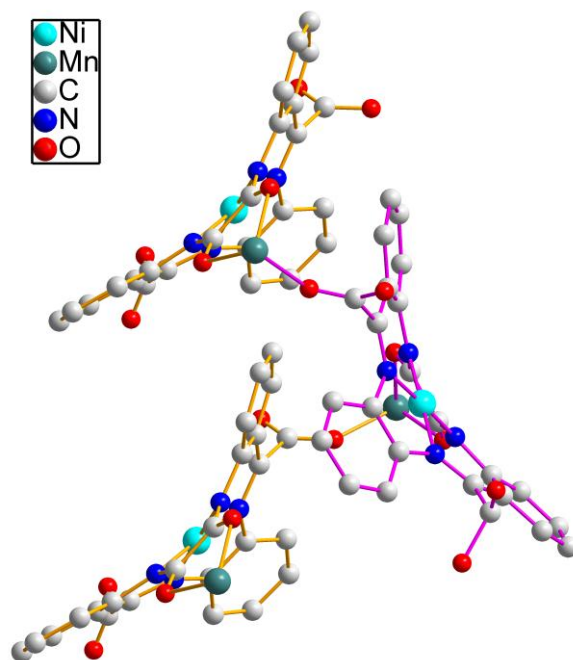


Fig. S10 Plot showing the $\pi \cdots \pi$ interactions between the adjacent NiL¹ ligands in a helical chain of **3**. (Hydrogen atoms and coordinated solvent molecules have been omitted for clarity.)

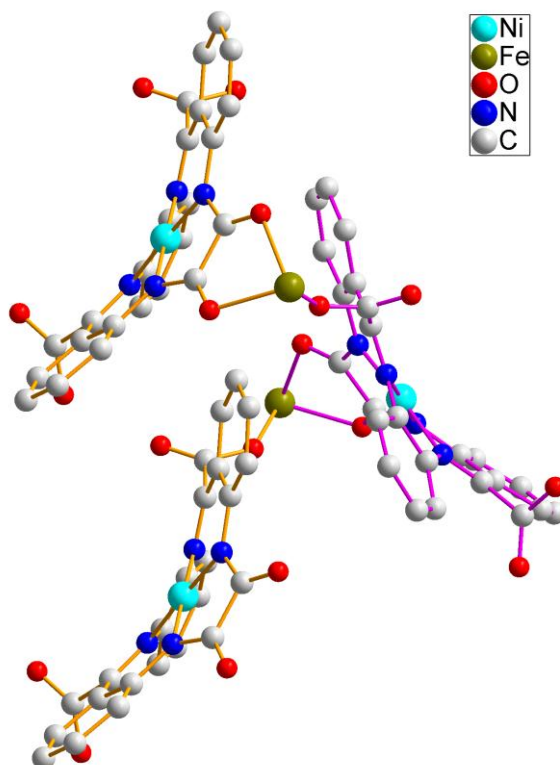


Fig. S11 Plot showing the $\pi \cdots \pi$ interactions between the adjacent NiL¹ ligands in a helical chain of Fe-NiL¹. (Hydrogen atoms and coordinated solvent molecules have been omitted for clarity.)

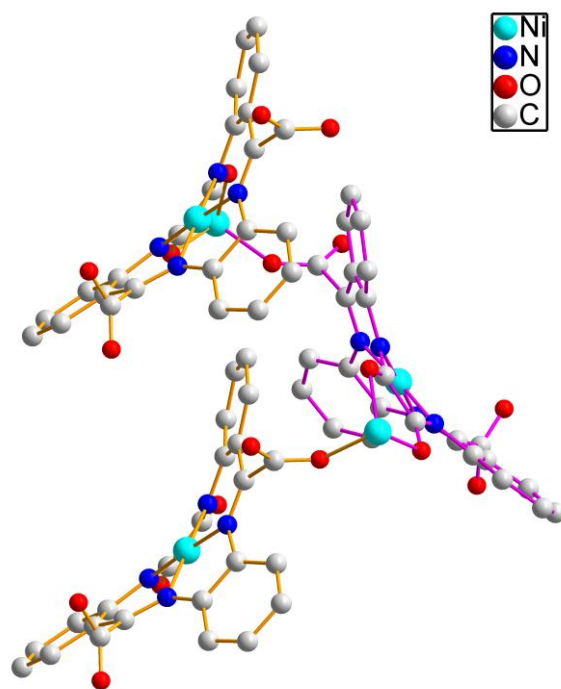


Fig. S12 Plot showing the $\pi \cdots \pi$ interactions between the adjacent NiL¹ ligands in a helical chain of Ni-NiL¹. (Hydrogen atoms and coordinated solvent molecules have been omitted for clarity.)

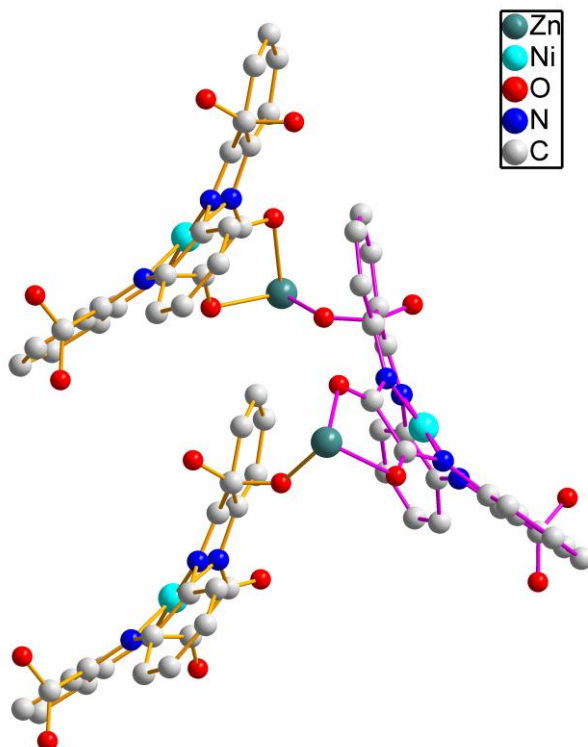


Fig. S13 Plot showing the $\pi \cdots \pi$ interactions between the adjacent NiL¹ ligands in a helical chain of Zn-NiL¹. (Hydrogen atoms and coordinated solvent molecules have been omitted for clarity.)

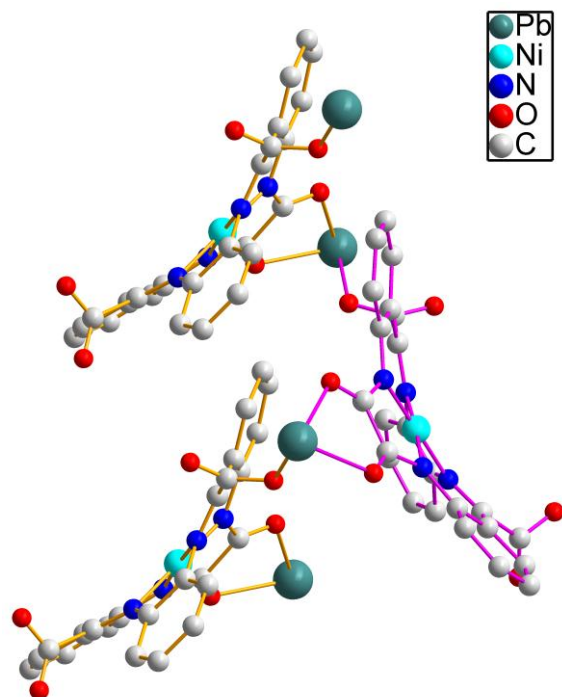


Fig. S14 Plot showing the $\pi \cdots \pi$ interactions between the adjacent NiL¹ ligands in a helical chain of Pb-NiL¹. (Hydrogen atoms and coordinated solvent molecules have been omitted for clarity.)

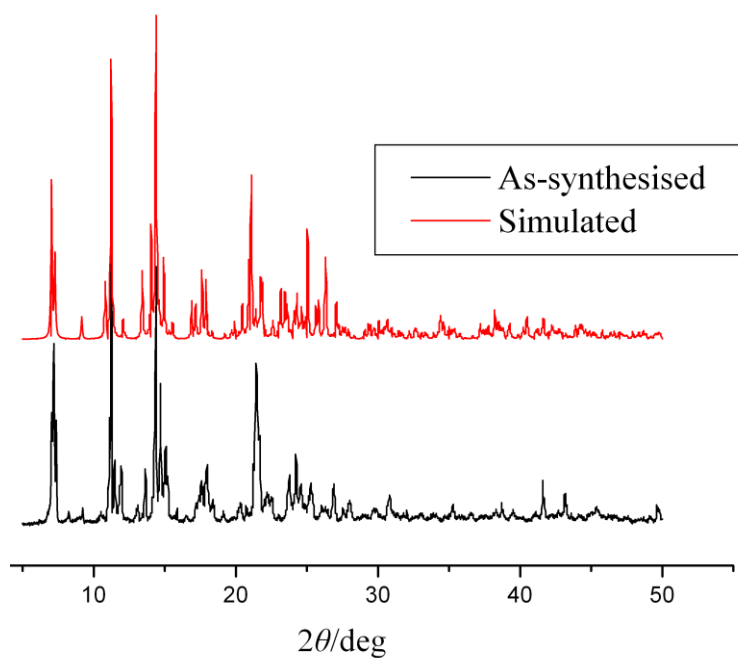


Fig. S15 PXRD patterns of **1** simulated from the X-ray single-crystal structure and as-synthesized samples.

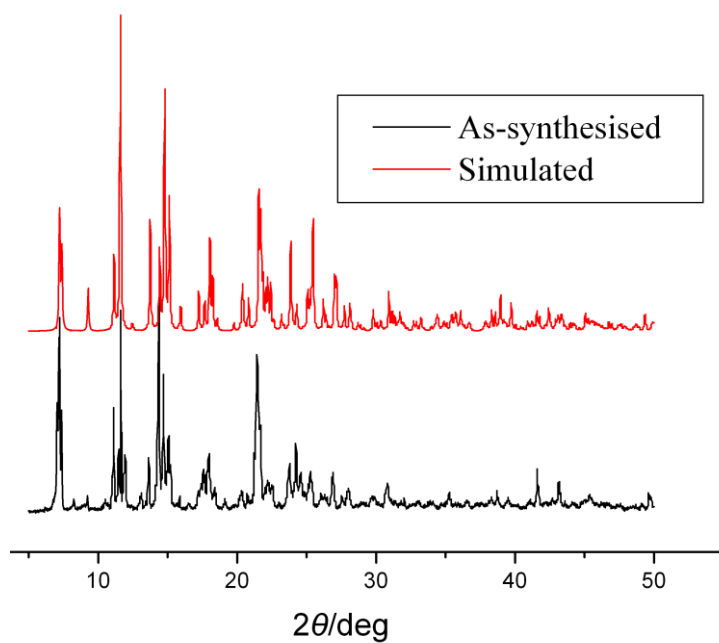


Fig. S16 PXRd patterns of **2** simulated from the X-ray single-crystal structure and as-synthesized samples.

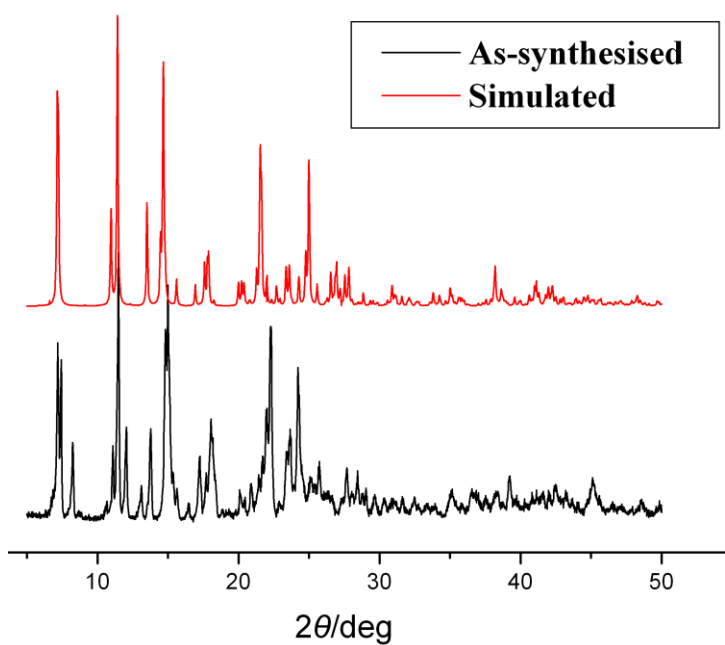


Fig. S17 PXRd patterns of **3** simulated from the X-ray single-crystal structure and as-synthesized samples.

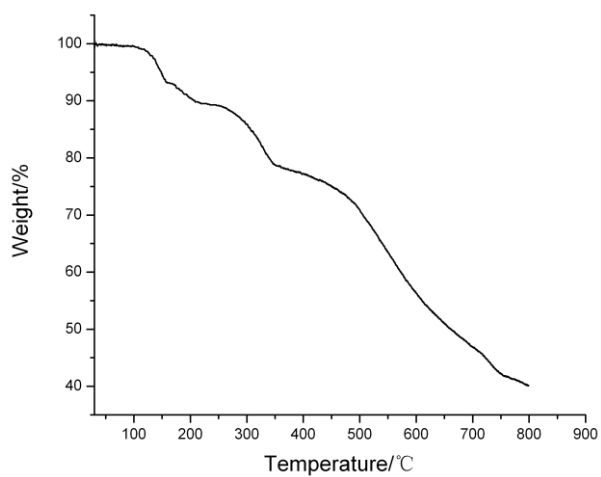


Fig. S18 TGA plot of **1**.

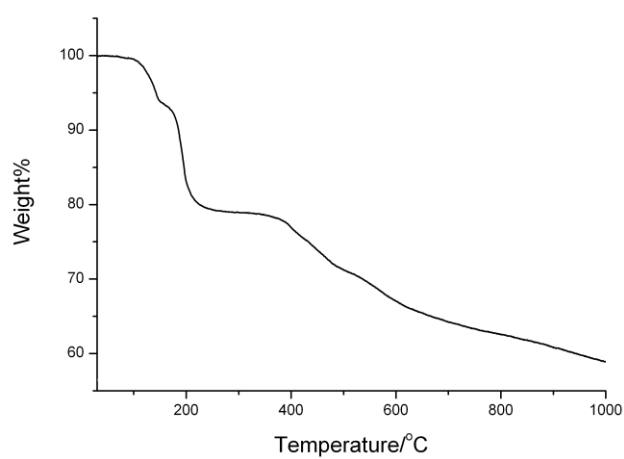


Fig. S19 TGA plot of **2**.

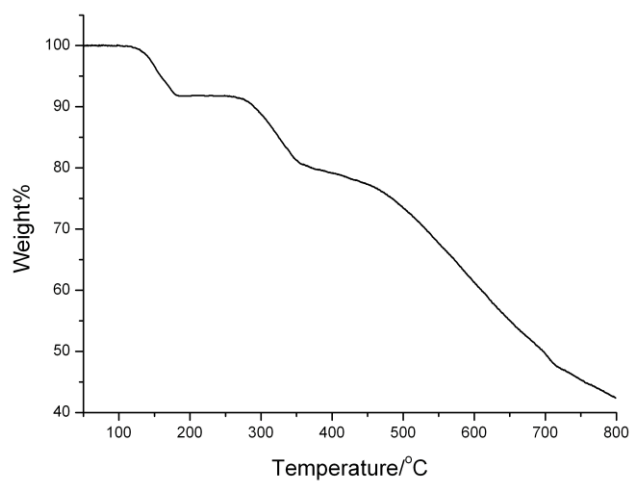


Fig. S20 TGA plot of **3**.